Sensor applications

Automatic Relevance Determination Kernel-Embedded Gaussian Process Regression for Sonar-Based Human Leg Localization with a Mobile Robot

Pritam Paral[1*], Saibal Ghosh[2], Amitava Chatterjee[2**], and Sankar K. Pal[1***]

[1] *Center for Soft Computing Research, Indian Statistical Institute (ISI), Kolkata 700108, India*
[2] *Department of Electrical Engineering, Jadavpur University, Kolkata 700032, India*
[*] *Member, IEEE*
[**] *Senior Member, IEEE*
[***] *Life Fellow, IEEE*

Manuscript received 25 October 2022; revised 21 November 2022; accepted 26 December 2022. Date of publication 29 December 2022; date of current version 19 January 2023.

Abstract—Human leg localization problems involving sonar sensing can be posed as a *nonlinear regression problem*, and, nonparametric Bayesian methods, such as the *Gaussian process regression* (GPR) model, are potential solution candidates. In this work, to overcome the problem of irrelevant input features from the sonar range data, an advanced *automatic relevance determination* kernel structure is proposed to be used in the GPR model instead of the commonly used standard isotropic kernel. It is able to extract high-relevance input features even from partially trained data, thus offering a better generalization ability while improving the prediction rates and robustness significantly.

Index Terms—Sensor applications, automatic relevance determination (ARD), Gaussian process regression (GPR), human leg localization (HLL), mobile robot, sonar sensing.

I. INTRODUCTION

The problems of detecting, identifying, and following moving people are considered a key problem in human–robot coexisting environments [1], [2], [3], [4]. In our recent work [5], we addressed a crucial subproblem within this genre, especially keeping in mind the constraints in developing countries, where the range readings obtained with the onboard sonar sensor of a mobile robot are used for human leg localization (HLL) in Cartesian coordinate space at different time instants, during a pursuit. The work successfully demonstrated how a sonar-based HLL problem can be solved as a *nonlinear regression problem* in which two distinct sets of observed data are used to learn two different prediction models [5]. The observed datasets include the same input data, i.e., 1) different angular positions of the human leg-pair with respect to (w.r.t) a specific robot pose and 2) sonar readings obtained at those angles but different output data, i.e., the corresponding x and y coordinates of the leg poses on the Cartesian plane. The learned models are then utilized to estimate the (x, y) coordinates for an unknown leg pose associated with an arbitrary input combination of angle and range information.

Considering sonar behavior [6], the HLL framework in [5] proposes to apply the *Gaussian process regression* (GPR) [7], [8] to effectively solve the regression problem formulated. The attractive analytical properties and tractable posterior computation ability of the *Gaussian process* (GP) make it a popular tool in various machine learning, signal processing, and statistical applications involving multiclass classification, identification, or nonlinear regression problems with real-world noise-corrupted data. In such cases, GPR turns out to be a robust and accurate nonparametric Bayesian method offering excellent resilience against *overfitting*.

Corresponding author: Pritam Paral (e-mail: callinpritam@gmail.com).
Associate Editor: F. Costa.
Digital Object Identifier 10.1109/LSENS.2022.3232920

However, unlike the classical GP, the GP model in [5] considered that the output data, i.e., (x, y) coordinates are certain and stable while the input data, i.e., angular orientations and ranges could suffer from uncertainty and imprecision. As the sonar positioning mechanism involved in [5] is servo motor driven, typical irregularities such as friction, dead zone, saturation, etc., occur frequently, which may affect the rotational movement of the sonar sensor induced via a specific set of software commands. This can very well infiltrate a certain extent of imprecision and uncertainty in the measurements of angular position and range data of the human legs. Conversely, the standard distance measurement methodology is adopted to measure the (x, y) coordinates on a real two-dimensional (2-D) plane, which leads to providing certain and reliable Cartesian positional data. Thus, the work in [5] essentially adapts the basic I/O properties of the standard GPR to carry out a statistical model calibration, used for estimating the leg positions in Cartesian space.

However, with the standard isotropic *squared exponential* (SE) kernel in GPR, the system suffers from irrelevant input features from the sonar range data. To deal with the same, we propose to replace the conventional isotropic SE kernel in GPR with the *Matern32* (M32) kernel having the structure of *automatic relevance determination* (ARD) [9]. This specific ARD structure becomes very useful in the case of independent priors over the length scales in the Gaussian covariance models. This ARD-based kernel works as a powerful tool for the extraction of discriminative input features from the entire data, as it judiciously eliminates irrelevant input features among orientation angles and range measurements by setting large length-scales for them [9]. Additionally, an advanced predictor with varied length-scales is developed to enhance the robustness and accuracy of predictions. To the best of our knowledge and belief, this work is the first to utilize ARD-based GPR models in the application of HLL using ultrasonic sensors.

Section II discusses GPR in brief. Section III presents the proposed HLL framework in light of the ARD kernel-based GPR. Section IV demonstrates the experimental results. Finally, Section V concludes the letter.

II. GLIMPSE OF GPR

The GP model is mainly used to learn an unknown function from a set of training data. Consider the following measurement model [10]:

$$z_k = \mathsf{f}(\mathbf{s}_k) + \varrho_k, \quad \varrho_k \sim \mathcal{N}(0,\ \mathsf{g}^2(\mathbf{s}_k)) \tag{1}$$

where $z_k \in \mathbb{R}$ denotes a noisy observation of the function $\mathsf{f}(\cdot)$ at the training point $\mathbf{s}_k \in \mathbb{R}^n$ of dimension n, and ϱ_k is the zero-mean measurement noise with variance $\mathsf{g}^2(\mathbf{s}_k)$. The objective is to learn a machine learning model for the predictive distribution of the target value z_Ω at a test location $\mathbf{s}_\Omega$, given an observed (training) dataset $\mathscr{D} = \{\mathbf{s}_k,\ z_k\}_{k=1}^{L}$. The measurements $\mathbf{z} = [z_1,\ z_2,\ \ldots,\ z_L]^T$ and the function value f_Ω are jointly Gaussian distributed as [10]

$$\begin{bmatrix} \mathbf{z} \\ \mathsf{f}_\Omega \end{bmatrix} \sim \mathcal{N}\left(\begin{bmatrix} \mathbf{0} \\ 0 \end{bmatrix}, \begin{bmatrix} \mathbf{C}+\mathbf{V} & \mathbf{C}_\Omega \\ \mathbf{C}_\Omega^{\mathsf{T}} & \mathsf{c}_{\Omega\Omega} \end{bmatrix}\right) \tag{2}$$

where $\mathbf{C}$ denotes the covariance matrix whose entries are $[\mathbf{C}]_{ij}$ computed from the covariance function $\mathsf{c}(\mathbf{s}_i,\ \mathbf{s}_j)$ at input locations $\mathbf{s}_i$ and $\mathbf{s}_j$, $\mathbf{C}_\Omega$ indicates the $L \times 1$ covariance matrix computed by $\mathsf{c}(\mathbf{s}_\Omega,\ \mathbf{s}_i)$ between test point $\mathbf{s}_\Omega$ and training point $\mathbf{s}_i$, $\mathbf{V}$ represents the diagonal matrix containing noise variances with elements: $[\mathbf{V}]_{ii} = \mathsf{g}^2(\mathbf{s}_i) = \mathsf{g}_i^2$, and $\mathsf{c}_{\Omega\Omega}$ denotes the prior variance computed from $\mathsf{c}(\mathbf{s}_\Omega,\ \mathbf{s}_\Omega)$ at $\mathbf{s}_\Omega$.

By putting a zero-mean GP prior over $\mathsf{f}(\cdot)$ and using the multivariate Gaussian distribution's analytical property, the conditional distribution that defines the posterior distribution of z_Ω [10] is obtained as follows:

$$p\,(z_\Omega|\mathbf{s}_\Omega,\ \mathbf{\Phi}_\mathsf{f},\ \mathbf{g},\ \mathsf{g}_\Omega,\ \mathscr{D}) \sim \mathcal{N}(\overline{z_\Omega},\ \mathsf{var}\,(z_\Omega)) \tag{3}$$

where $\mathbf{g} = [\mathsf{g}_1,\ \mathsf{g}_2,\ \ldots,\ \mathsf{g}_P]^T$ and g_Ω, respectively, represent the noise standard deviations at training points $S = [\mathbf{s}_1,\ \mathbf{s}_2,\ \ldots,\ \mathbf{s}_P]^T$ and test point $\mathbf{s}_\Omega$, $\mathbf{\Phi}_\mathsf{f}$ denotes the hyperparameters of the covariance function, and $\overline{z_\Omega}$ and $\mathsf{var}(z_\Omega)$, respectively, denote the posterior mean and variance of the test output z_Ω, which are expressed as [10]

$$\overline{z_\Omega} = \mathbf{C}_\Omega^{\mathsf{T}}(\mathbf{C}+\mathbf{V})^{-1}\mathbf{z} \tag{4}$$

$$\mathsf{var}\,(z_\Omega) = \left\{\mathsf{c}_{\Omega\Omega} - \mathbf{C}_\Omega^{\mathsf{T}}(\mathbf{C}+\mathbf{V})^{-1}\mathbf{C}_\Omega\right\} + \mathsf{g}_\Omega^2. \tag{5}$$

The conditional mean $\overline{z_\Omega}$ is designated as the *best estimate* while conditional variance $\mathsf{var}(z_\Omega)$ captures the uncertainty in the estimate.

III. HUMAN LEG-PAIR LOCALIZATION FRAMEWORK

A. Mode of Data Acquisition

During the pursuit, a set of sonar readings is acquired for the target leg-poses at a certain time instant, and with these data, it is aimed to estimate the leg positions on the Cartesian plane at that time instant.

Following the same framework of data acquisition as in [5], two different sets of data are generated in this work as well. Each of them contains the same input information, i.e., the angular orientations of several human leg postures w.r.t a specific robotic pose and the range measurements captured at those orientation angles. However, both the datasets comprise different output information consisting of the corresponding x and y coordinates of the target leg postures, respectively. The *reference position* of the robot is considered $(0,\ 0)$ on a horizontal 2-D plane and the robot heading is taken along the $+y$-axis direction. A set of range measurements $\tilde{r}_{D_j} \approx r_D|_{j=1}^{P}$ are acquired for different leg poses of a target person while he/she is located around a radial proximity of r_D along a predefined set of equidistant angles $\phi_j \in [0^\circ,\ 180^\circ]|_{j=1}^{P}$ [5]. Simultaneously, the true values of corresponding leg positions are measured on the 2-D coordinate plane by the conventional line gauge-based direct distance measurement technique [5]. A set of N different radial distances $\{r_D^{(k)}\}_{k=1}^{N}$ are considered, thus generating a total $M = N * P$ number of different $\{\tilde{r}_D,\ \phi\}$ polar coordinates. With an equal number of Cartesian measurements, the combinations of polar and Cartesian parameters are populated in two separate datasets as [5]

$$\mathscr{D}_1 = \{(r_k, \theta_k),\ x_k\}_{k=1}^{M}; \quad \mathscr{D}_2 = \{(r_k, \theta_k),\ y_k\}_{k=1}^{M} \tag{6}$$

with $r_{(N-1)P+1} = \tilde{r}_{D_1}^{(N)},\ \theta_{(N-1)P+1} = \phi_1, \ldots, r_{NP} = \tilde{r}_{D_P}^{(N)},\ \theta_{NP} = \phi_P$.

Similar to [5], while acquiring the range data for the leg-pair located around $r_D^{(m)}$ in a specific angular direction ϕ_k, a set of sonar readings, rather than a single one, are gathered by the onboard sonar configuration with a 180° *field of view*. This is done primarily to curb the sonar uncertainty in the process of range data acquisition. However, while generating datasets in our formulated regression problem, only single-range inputs are accepted correspond to individual angular instances. Therefore, taking into account the sonar imprecision, an error-tolerant equivalent range reading $\tilde{r}_{D_k}^{(m)}$ along angle ϕ_k is generated. The averaging mechanism for obtaining $\tilde{r}_{D_k}^{(m)}$ is detailed in [5]. The scheme for acquiring sonar readings for a specific leg pose along a particular angle is exemplified in Fig. 1.

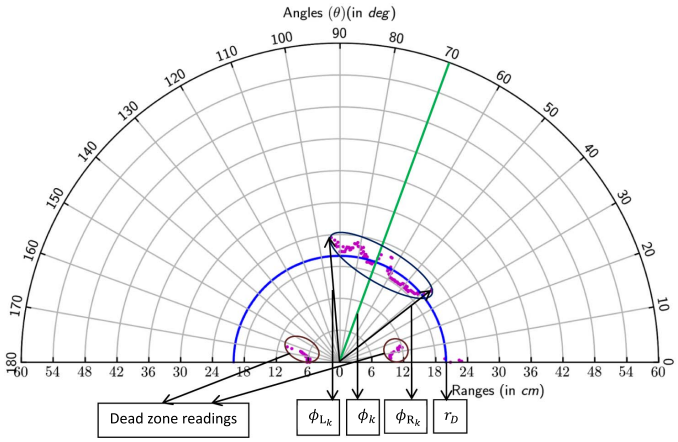

Fig. 1. Gathering sonar readings for the leg-pair located around r_D in the angular direction ϕ_k, with $\phi_k = 70^\circ$ and $r_D = 20$ cm. *Magenta* points represent the sonar readings. ϕ_{L_k} and ϕ_{R_k}, respectively, are the angles of the left-most and right-most range readings detected [5].

B. Proposed Leg Localization Model

Similar to [5], in the present regression-based HLL model, two distinct training datasets $\mathscr{D}_1 = \{\mathbf{v}_k,\ x_k\}_{k=1}^{M}$ and $\mathscr{D}_2 = \{\mathbf{v}_k,\ y_k\}_{k=1}^{M}$ are used to learn two different prediction models, best described via the unknown functions $\mathsf{X} : \mathbb{R}^2 \to \mathbb{R}$ and $\mathsf{Y} : \mathbb{R}^2 \to \mathbb{R}$, respectively. With $\mathbf{v}_k = [r_k, \theta_k] \in \mathbb{R}^2$ being the *two*-dimensional input vector, the measured scalar outputs $x_k,\ y_k \in \mathbb{R}$ can be approximated as [5]

$$\begin{aligned} x_k &= \mathsf{X}(\mathbf{v}_k) + \varrho_{xk} \quad \varrho_{xk} \sim \mathcal{N}(0,\ \mathsf{g}_x^2(\mathbf{v}_k)) \\ y_k &= \mathsf{Y}(\mathbf{v}_k) + \varrho_{yk} \quad \varrho_{yk} \sim \mathcal{N}(0,\ \mathsf{g}_y^2(\mathbf{v}_k)). \end{aligned} \tag{7}$$

The error terms ϱ_{xk} and ϱ_{yk}, referred to as the *equivalent modeling errors* (EMEs), have been introduced to take the measurement uncertainties into account. The EMEs, primarily resulting from the uncertainties in input variables, can be considered independent and normally distributed random variables, as discussed in [5]. The noise variances, defined as $\mathsf{g}_x^2(\mathbf{v}) \equiv \beta_{nx}^2$ and $\mathsf{g}_y^2(\mathbf{v}) \equiv \beta_{ny}^2$, are assumed to remain constant across the input space. For M number of observed instances, we define $\mathbf{g}_x = [\mathsf{g}_{x1}, \ldots, \mathsf{g}_{xM}]^{\mathsf{T}}$ with $\mathsf{g}_{xk} = \mathsf{g}_x(\mathbf{v}_k)$. Now, for a given unknown leg posture associated with input $\mathbf{v}_\Omega = [r_\Omega, \theta_\Omega]$, these two learned models can be used to localize the $(x_\Omega,\ y_\Omega)$ coordinates of the corresponding leg posture w.r.t the robotic reference

frame [5]. Typically, the unknown polar parameter $\mathbf{v}_\Omega = [r_\Omega, \theta_\Omega]$ does not coincide with the predefined set of parameters $\mathbf{v}_k = [r_k, \theta_k]|_{k=1}^M$, and thus x_Ω and y_Ω are, in general, unknown, which are required to be estimated from known variables $\{x_k\}_{k=1}^M$, $\{y_k\}_{k=1}^M$.

Similar to [5], the GPR is proposed to be applied in our present leg localization problem with the aim of predicting the unknown Cartesian coordinates x_Ω and y_Ω corresponding to a query input $\mathbf{v}_\Omega = [r_\Omega, \theta_\Omega]$, given two distinct sets of observed data $[x_1, x_2, \ldots, x_M]^\mathsf{T}$ and $[y_1, y_2, \ldots, y_M]^\mathsf{T}$ at hand for the corresponding polar inputs $\mathbf{v}_1, \mathbf{v}_2, \ldots, \mathbf{v}_M$ [5]. Following the same approach of estimating the target output z_Ω for a test input $\mathbf{s}_\Omega$, as illustrated in Section II, both x_Ω and y_Ω for $\mathbf{v}_\Omega$ can be estimated with $\mathsf{g}_x^2(\mathbf{v}_\Omega) = \beta_{nx}^2$ and $\mathsf{g}_y^2(\mathbf{v}_\Omega) = \beta_{ny}^2$.

C. GPR Kernel Functions With ARD Structure

In our previous work [5], the popular SE kernel was adopted as the covariance function, which is given by [8]

$$\mathsf{c}_{\mathsf{SE}}(\mathbf{v}, \mathbf{v}') = \alpha_{\mathsf{SE}}^2 \exp\left[-\|\mathbf{v} - \mathbf{v}'\|^2 / \left(2\gamma_{\mathsf{SE}}^2\right)\right] \tag{8}$$

with $\|\cdot\|$, α_{SE}, and γ_{SE}, respectively, denoting the Euclidean distance between input points $\mathbf{v}$ and $\mathbf{v}'$, the signal amplitude, and the characteristic length-scale. The hyperparameters α_{SE} and γ_{SE} are typically denoted as $\mathbf{\Phi}_{\mathsf{SE}} = \{\alpha_{\mathsf{SE}}, \gamma_{\mathsf{SE}}\}$. SE kernel is a *stationary* kernel in which the correlations between various points are solely influenced by the term $\mathbf{v} - \mathbf{v}'$, resulting in a smooth distribution. For sonar range data with numerous local fluctuations, this would be too strict. Therefore, in this work, *Matern32* (M32) kernel is selected over the SE kernel, which is expressed as [9]

$$\mathsf{c}_{\mathsf{M32}}(\mathbf{v}, \mathbf{v}') = \alpha_{\mathsf{M32}}^2 \left[1 + \frac{\sqrt{3}\|\mathbf{v} - \mathbf{v}'\|}{\gamma_{\mathsf{M32}}}\right] \exp\left[-\frac{\sqrt{3}\|\mathbf{v} - \mathbf{v}'\|}{\gamma_{\mathsf{M32}}}\right] \tag{9}$$

where the hyperparameters α_{M32} and γ_{M32}, respectively, involved in controlling the function amplitude and smoothness, are typically represented as $\mathbf{\Phi}_{\mathsf{M32}} = \{\alpha_{\mathsf{M32}}, \gamma_{\mathsf{M32}}\}$.

In real applications, the restricted capture ability of the isotropic kernels, such as the SE and M32 functions, would cause them to produce unreliable or incorrect predictions for nonlinear mapping involving multidimensional input variables. For our HLL model, the inputs contain the angular orientation terms, as well as the corresponding range measurements, and to extract these features and enhance accuracy, the ARD structure is embedded into the isotropic M32 kernels, as given by (10) and (11) [9]

$$\mathsf{c}_{\mathsf{M32+ARD}}(\mathbf{v}, \mathbf{v}') = \alpha_{\mathsf{M32}}^2 (1 + \sqrt{3\rho}) \exp\left[-\sqrt{3\rho}\right] \tag{10}$$

with

$$\mathbf{v} = [r, \theta]; \quad \mathbf{v}' = [r,' \theta']; \quad \rho = \frac{\|r - r'\|^2}{\gamma_r^2} + \frac{\|\theta - \theta'\|^2}{\gamma_\theta^2} \tag{11}$$

where r and r' are, respectively, the range readings in the directions θ and θ'. The hyperparameters γ_r and γ_θ, respectively, determine the relevancies of range and angle inputs w.r.t the regression results. A large value, in general, results in low relevancy. In the context of GPR, "learning" refers to the optimization of GP hyperparameters, including kernel hyperparameters and constant noise variance, by using the training dataset. In this work, *Limited-memory Broyden–Fletcher–Goldfarb–Shanno* (L-BFGS) algorithm [12] is employed to fit the GP hyperparameters through the maximization of log-marginal likelihood (LML) [11]. Fig. 2 shows the functional diagram of our ARD kernel-based approach.

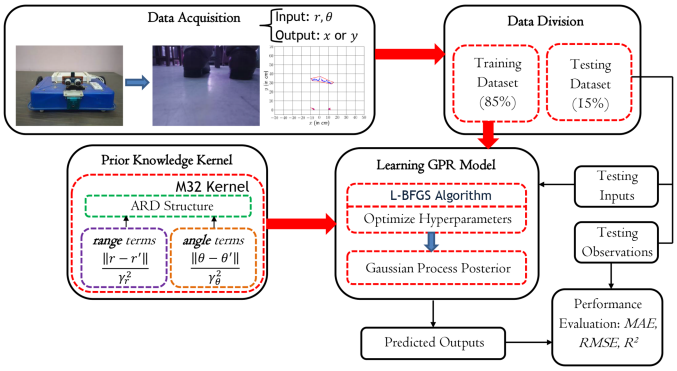

Fig. 2. Functional diagram of the ARD kernel-based HLL approach.

IV. EXPERIMENTAL RESULTS

A. Experimental Setup

For the purpose of performance evaluation, we use the real sonar data acquired by the onboard HC-SR04 ultrasonic sensor of an economical, indigenously developed, two-wheel differentially driven mobile robot based on Raspberry Pi 3 model B+ [4]. Two real-world datasets $\mathscr{D}_1 = \{(r_k, \theta_k), x_k\}_{k=1}^M$ and $\mathscr{D}_2 = \{(r_k, \theta_k), y_k\}_{k=1}^M$ are formed for different positions of human leg-pair in polar coordinate space. Assuming the sonar range is valid in the interval (5, 55) cm, the radial distances $\{r_D^{(k)}\}_{k=1}^N$ are chosen as {5 cm, 7 cm, ..., 53 cm, 55 cm} while the angles $\{\phi_j\}_{j=1}^P$ are adopted as $\{10^\circ, 20^\circ, \ldots, 160^\circ, 170^\circ\}$ (considering *dead zone* nonlinearity). The parameters N, P, and M are, respectively, 26, 17, and 442. The training/testing is performed with 85%/15% training-testing split.

B. Performance Evaluations

The estimation performance of the proposed ARD-kernel-based HLL approach (called HLL-M32+ARD) is assessed by means of *three* quantitative metrics: *root mean square error* (RMSE), *mean absolute error* (MAE), and *fit-goodness* (R^2) between the ground-truth observations and predicted outputs [9], and is compared with our earlier SE-kernel-based HLL approach [5] (called HLL-SE), and the conventional (r, θ) to (x, y) conversion method. As evidenced by Table 1, HLL-M32+ARD outperforms HLL-SE and the conventional method in estimating x and y positions, uniformly for all three metrics.

To demonstrate the effectiveness of HLL-M32+ARD, two representative cases are illustrated in Fig. 3, where estimation results for y coordinates achieved by two competing GPR-based approaches are presented. In the first case, the range measurements are varied by keeping the orientation angle fixed at a certain value [see Fig. 3(a) and (b)], whereas in the second case, the angle inputs are varied around a specific radial distance [see Fig. 3(c) and (d)]. To describe and summarize the uncertainty related to the estimation of unknown parameters, credible intervals are used, which are especially pertinent in the context of the empirical Bayesian framework [13]. As can be observed from Fig. 3(a) and (c), the mean estimation results obtained with HLL-SE get closer to the real data. The corresponding 95% credible intervals, however, show wide distributions, which implies that high uncertainty is attained in these cases. This degradation in the estimation performance is primarily induced by the overfitting problem, implying that the solo kernel structure has a limited capability of generalization. With reference to Fig. 3(b) and (d), HLL-M32+ARD shows improved mean estimation over HLL-SE and, more importantly,

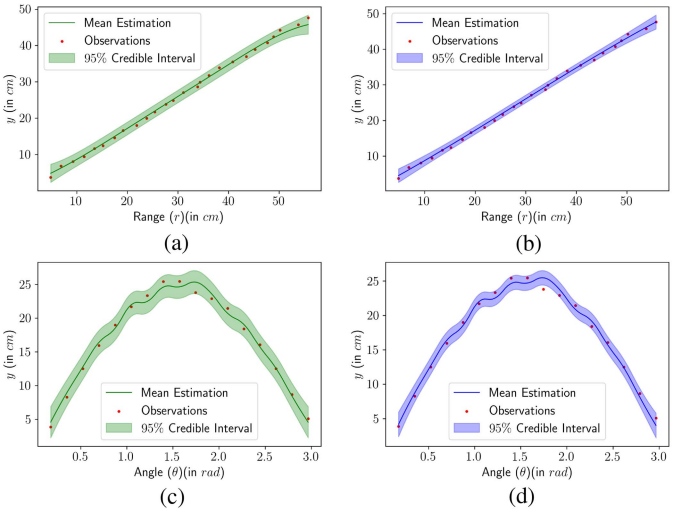

Fig. 3. Estimation results for y coordinates obtained from (a) HLL-SE and (b) HLL-M32+ARD with range measurements being varied at orientation angle 60°; (c) HLL-SE and (d) HLL-M32+ARD with angle inputs being varied around radial distance 25 cm.

TABLE 1. Comparison of Quantitative Metrics Among the Conventional Method, HLL-SE, and HLL-M32+ARD in Estimating x and y

Method	Estimation of x			Estimation of y		
	RMSE (in m)	MAE (in m)	R^2	RMSE (in m)	MAE (in m)	R^2
Conventional Approach	0.0275	0.0231	0.9803	0.0261	0.0210	0.9617
HLL-SE	0.0075	0.0061	0.9958	0.0081	0.0063	0.9934
HLL-M32+ARD	**0.0067**	**0.0055**	**0.9989**	**0.0063**	**0.0048**	**0.9977**

The bold values represent the best results obtained with the competing methods corresponding to three performance metrics.

95% credible intervals for HLL-M32+ARD distribute in considerably narrower regions, indicating that it achieves much higher estimation credibility and lower uncertainty compared to HLL-SE. This impressive performance of HLL-M32+ARD can be attributed to the strong feature extraction capabilities of the ARD structure, in addition to the high robustness offered by the M32 kernel. The ARD kernel with variable length-scales can effectively learn the relevance of the input features and subsequently remove irrelevant features by setting large length-scales for them. This allows for the retention of only the input features modeling the underlying structure of the observed data rather than the noise so that overfitting is alleviated.

To study the effects of the variation of γ_r and γ_θ on LML (logarithmic evidence) [11], surface plots are generated corresponding to the processes of learning prediction models for x and y positions. The corresponding plots, shown in Fig. 4(a) and (c), respectively, help to provide independent verification of the optimization results obtained from L-BFGS algorithm.

V. CONCLUSION

An advanced HLL model based on GPR is proposed that deals with a major issue of irrelevant input features associated with real-world sonar data. Inappropriate input features can cause erroneous learning

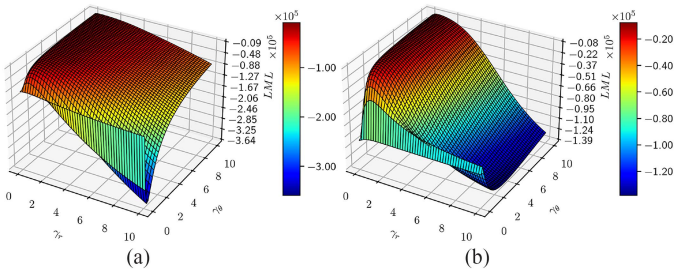

Fig. 4. Effects of variation of length-scales γ_r and γ_θ on LML with unity signal amplitude ($\alpha_{\text{M32}} = 1$): In the processes of learning prediction models for (a) x and (b) y positions.

of a regression-based prediction model. With the ARD-based kernel structure, the proposed GPR-based approach can robustly learn the prediction models by effectively eliminating irrelevant input features and localize the $(x,\ y)$ coordinates of query leg postures with enhanced accuracy. Real-life performance evaluations aptly demonstrate the superiority of our ARD kernel-based approach.

ACKNOWLEDGMENT

Prof. S. K. Pal acknowledges the National Science Chair, SERB-DST, GoI.

REFERENCES

[1] J. Yuan, H. Chen, F. Sun, and Y. Huang, "Multisensor information fusion for people tracking with a mobile robot: A particle filtering approach," *IEEE Trans. Instrum. Meas.*, vol. 64, no. 9, pp. 2427–2442, Sep. 2015.

[2] P. Paral, A. Chatterjee, and A. Rakshit, "Vision sensor-based shoe detection for human tracking in a human–robot coexisting environment: A photometric invariant approach using DBSCAN algorithm," *IEEE Sens. J.*, vol. 19, no. 12, pp. 4549–4559, Jun. 2019.

[3] D. Li, L. Li, Y. Li, F. Yang, and X. Zuo, "A multi-type features method for leg detection in 2-D laser range data," *IEEE Sens. J.*, vol. 18, no. 4, pp. 1675–1684, Feb. 2018.

[4] P. Paral, A. Chatterjee, and A. Rakshit, "Human position estimation based on filtered sonar scan matching: A novel localization approach using DENCLUE," *IEEE Sens. J.*, vol. 21, no. 6, pp. 8055–8064, Mar. 2021.

[5] P. Paral, A. Chatterjee, and A. Rakshit, "Sonar sensing-based human leg localization using Gaussian process regression," in *Advances in Intelligent Systems and Computing*, K.-K. Giri et al., Eds. Berlin, Germany: Springer, 2022, vol. 1412, pp. 1029–1041.

[6] A. Burguera, Y. González, and G. Oliver, "On the use of likelihood fields to perform sonar scan matching localization," *Auton. Robot.*, vol. 26, no. 4, pp. 203–222, May 2009.

[7] C. M. Bishop, *Pattern Recognition and Machine Learning*. 1st ed. Berlin, Germany: Springer, 2006.

[8] S. Lee and J. McBride, "Extended object tracking via positive and negative information fusion," *IEEE Trans. Signal Process.*, vol. 67, no. 7, pp. 1812–1823, Apr. 2019.

[9] K. Liu, Y. Li, X. Hu, M. Lucu, and W. D. Widanage, "Gaussian process regression with automatic relevance determination kernel for calendar aging prediction of lithium-ion batteries," *IEEE Trans. Ind. Informat.*, vol. 16, no. 6, pp. 3767–3777, Jun. 2020.

[10] Q.-H. Zhang and Y.-Q. Ni, "Improved most likely heteroscedastic Gaussian process regression via Bayesian residual moment estimator," *IEEE Trans. Signal Process.*, vol. 68, pp. 3450–3460, May 2020.

[11] C. K. Williams and C. E. Rasmussen, *Gaussian Processes for Machine Learning*, vol. 2, Cambridge, MA, USA: MIT Press, 2006.

[12] J. Nocedal and S. J. Wright, *Numerical Optimization*, 2nd ed. New York, NY, USA: Springer, 2006.

[13] D. Makowski, M. S. Ben-Shachar, and D. Lüdecke, "bayestestR: Describing effects and their uncertainty, existence and significance within the Bayesian framework," *J. Open Source Softw.*, vol. 4, no. 44, Aug. 2019, Art. no. 1541.